# PHBV Crystallization under Injection Molding Conditions: Influence of Packing Pressure and Mold Temperature

G. El hajj Sleiman[1], G. Colomines[1], R. Deterre[1], I. Petit[1], E. Leroy[2] and S. Belhabib[1,*]

[1]UBL, IUT Nantes, CNRS, GEPEA, UMR 6144, OPERP, 2 Avenue du professeur Jean ROUXEL, BP 539, 44475 Carquefou, France
[2]UBL, CNRS, GEPEA, UMR 6144, CRTT, 37, Boulevard de l'Université, 44606 St Nazaire Cedex, France

**ABSTRACT:** Poly(3-hydroxy butyrate)-co-(3-hydroxy valerate) (PHBV) is a biobased and biodegradable polyester. This semicrystalline bioplastic could be a good candidate for the replacement of some commodity plastics derived from oil. However, the control of the conditions of its processing in order to obtain optimal properties of the finished products remains a current research subject. The objective of this work is to better understand the crystallization under injection molding conditions by inline measurements during the process. We focused on the influence of two key processing parameters, namely, mold temperature and packing pressure. The modeling of inline temperature measurements allowed an inverse estimation of the thermodynamic melting temperature of PHBV and of the heat of crystallization's variations with processing parameters.

**KEYWORDS:** Crystallization, PHBV, injection molding, inline measurement

## 1 INTRODUCTION

Over the recent decades, poly(hydroxyl alcanoates) (PHAs) have drawn a lot of attention as a family of biobased and biodegradable polyesters produced by microorganisms, whose chemical structure and properties can be controlled by biotechnology [1]. However, commercial PHAs, such as Poly(3-hydroxy butyrate)-co-(3-hydroxy valerate) (PHBV), still have limited applications. Besides still being relatively high price, PHAs suffer from a poor thermal stability under melt processing conditions [2] and from progressive embrittlement after processing due to physical aging and secondary crystallization [3]. These issues can be respectively addressed by using the so-called reverse temperature profile in injection molding [4] and by optimizing the primary crystallization [3]. For that reason, important research efforts have been dedicated to the influence of nucleating agents [5–6], including nanoparticles [7–8], and to crystallization kinetics studies both under isothermal [8–11] and non-isothermal conditions [12–13]. However, these studies have generally been based on differential scanning calorimetry experiments. Contrary to conventional semicrystalline plastics such as polyolefin, no experimental studies of

the crystallization of PHAs under real processing conditions can be found in the literature. To our knowledge, only numerical simulations of molded PHBV part crystallization upon cooling were performed [14].

In the present paper, we use a specific experimental design previously developed by our research group for inline characterization of polypropylene crystallization kinetics under injection molding conditions [15]. This device allows investigating the influence of two key processing parameters, namely, mold temperature and packing pressure, on PHBV crystallization kinetics.

## 2 EXPERIMENTAL AND MODELING

### 2.1 Materials

A poly(3-hydroxybutyrate-co-3-hydroxyvalerate) (PHBV) produced by Tianan Biologic (China) for injection molding (Grade Y1000P) was used. According to the supplier, it has a melting temperature of 165 °C and contains a nucleating agent of unknown nature. Before processing, it was dried following the supplier's recommendations (48 h at 95 °C in order to obtain a moisture content below 250 ppm, measured by the Karl Fischer method).
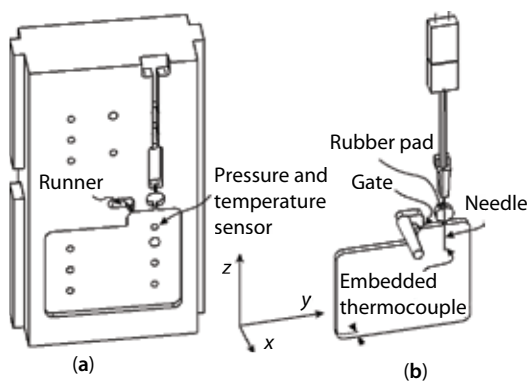
## 2.2   Injection Molding and Inline Temperature Measurements

A Milacron Elektron 50 injection molding machine equipped with an instrumented molding cavity (Figure 1) was used. The barrel temperature was set to 180 °C, with a melt residence time of 20 s before injection (40 mm/min; 700 bar). Note that according to our previous work on PHBV thermomechanical degradation under injection molding conditions [2], these real processing conditions are expected to lead to a decrease of PHBV molecular masses. This may affect crystallization kinetics in a way that is not detectable by offline studies by DSC on pristine PHBV.

After injection, a pressure holding time of 30 s and a total cooling time of 40 s were used before opening the mold. Two different mold temperatures (30 °C and 60 °C) and two different holding pressures (100 bar and 200 bar) were used. The molding cavity (Figure 1) is instrumented with two pressure-temperature sensors (diameter 4 mm; Kistler©) located opposite each other in the mobile and fixed parts of the mold. A flying probe designed and described in detail in previous works [15–16] allows monitoring the temperature inside the polymer during cooling and crystallization. Briefly, it consists of a K-type thermocouple (butt-welded chromel-alumel filament of diameter 50 μm, allowing a measuring range up to 1100 °C, with typical accuracy of ± 0.2%). The thermocouple is positioned in the middle of the molding cavity's thickness (4 mm) thanks to a needle which also allows its protection and prevents motion under the effect of the holding pressure (Figure 1).

The position of the thermocouple is determined *a posteriori* after each injection molding experiment. This is done by cutting the injected part closest to the thermocouple. Then, the part containing the thermocouple tip is polished until the thermocouple becomes clearly visible. A binocular microscope is then used to capture
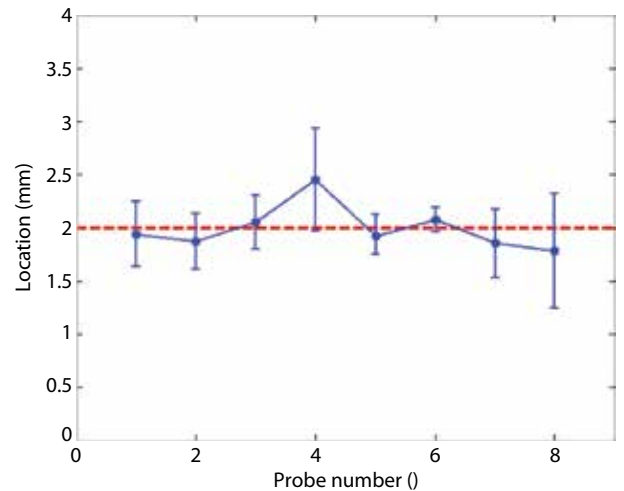
an image of the thickness with the thermocouple position. Figure 2 shows the distribution of the thermocouple positions obtained inside the 4 mm thick molded parts in a series of injection molding experiments.

## 2.3   Modeling and Simulation of Flying Probe Temperature Evolution

Our objective was to simulate the temperature of PHBV at the center of the molding cavity measured with the flying probe during cooling stage. The ejection step where the molded part is in contact with ambient air outside the mold, is not modeled in the present study.

Because the thickness of the molded part (4 mm) is much smaller than its width (81 mm) and height (71 mm) (Figure 1), the heat transfers in the thickness dimension are predominant. Thus, a one-dimensional heat transfer problem in the thickness direction x was considered (Figure 3).

At the end of the mold filling step ($t = 0$), the molten polymer and the mold temperatures are considered homogeneous and are respectively equal to the



**Figure 2** Distribution of flying temperature probe thermocouple positions for the different injected samples (location around 2 mm, in the center of the mold cavity).



**Figure 1** Instrumented molding cavity (**a**) and flying temperature probe (**b**).
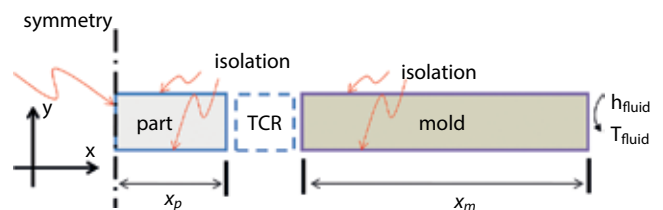


**Figure 3** One-dimensional heat transfer problem in the thickness direction x.

injection temperature ($T_{inj}$) and the set cooling temperature ($T_{mold}$) controlled by the injection molding machine's thermoregulator. The polymer in the mold is assumed immobile, thereby neglecting the effect of the viscosity.

The 4 mm thick molded PHBV part is situated between two thick steel blocks of 24 mm thickness (Figure 3). Because the boundary conditions are identical on both sides of the molded part; simulating the cooling of the injected part is reduced to a symmetric problem. Before opening the mold, the thermal transfer mode between the part and the mold is conduction-type. The PHBV part is in contact with both parts of the mold, the temperature of which is regulated by the cooling channels to the set temperature $T_{fluid}$ with a $h_{fluid}$ exchange coefficient between the mold and the fluid.

Cooling of the PHBV part is described by the heat equation with a source term, taking into account the heat generated during crystallization:

$$\frac{Cp(T,a)}{v(P,T,a)}\frac{\partial T}{\partial t} + \nabla\left(-\lambda(T,a).\nabla T\right) - \frac{\Delta H}{v(P,T,a)}\frac{\partial a}{\partial t} = 0$$

(1)

where $Cp(T, a)$, $\lambda(T, a)$, and $v(P, T, a)$ are the thermophysical properties of the polymer: heat capacity, heat conductivity, and specific volume, respectively, and $\Delta H$ is the latent heat of crystallization.

It is noteworthy that the value of $\Delta H$ actually depends on the absolute crystallinity degree at the end of the cooling step. As an opposition, $a$ is the relative crystallinity degree defined as follows: $a = 0$ corresponds to the initial molten state, and $a = 1$ corresponds to the final semicrystalline state at the end of cooling. Depending on cooling and crystallization kinetics, this final absolute crystallinity degree corresponds to $a = 1$, and so the value of $\Delta H$ can vary. However, the only simulations available for PHBV in the literature consider a fixed value of $\Delta H$ [14]. In the present work, we will use this fixed value of $\Delta H$ as a first approximation, but we will show that the variations of $\Delta H$, depending on processing conditions, can also be evaluated by inverse estimation.

Despite the heat capacity, heat conductivity and specific volume can depend on temperature $T$, pressure P and relative crystallinity $\alpha$, the thermal conductivity and the specific volume were considered constant, and the pressure dependence was neglected. For the heat capacity:

$$Cp(T,a) = (1-a)\cdot Cp_a(T) + a\cdot Cp_{sc}(T)$$

(2)

where $Cp_a$ and $Cp_{sc}$ are heat capacity for PHBV in amorphous/melt and final semicrystalline states.

Given that the well-known Avrami model only suitably describes isothermal crystallization kinetics [10, 17], the Nakamura law [18] which is best suited for non-isothermal crystallization kinetics modeling was used:

$$\frac{\partial a}{\partial t} = n\kappa(T)(1-a)\left(ln\left(\frac{1}{1-a}\right)\right)^{\frac{n-1}{n}}$$

(3)

where $n$ is similar to the Avrami parameter and $\kappa(T)$ is the rate constant, given by the crystallization theory of Hoffman-Lauritzen:

$$\kappa(T) = G_0 \cdot e^{\left(-\frac{U^*}{R(T-T_\infty)}\right)} \cdot e^{\left(-\frac{k_g}{T(T_{m0}-T)}\right)}$$

(4)

where $G_0$ is a pre-exponential coefficient that is considered here to be constant, $U^*$ represents the activation energy; $R$ is the universal constant of ideal gas; $K_g$ is the nucleating parameter relating to the energy required for the formation of a critically sized germ; $T_\infty = T_g - 30$ °C presents the temperature below which it is assumed that no movement of macromolecular chains can occur; $T_g$ is the glass transition temperature and $T_{m_o}$ is the thermodynamic melting temperature.

Concurrently, the heat transfer in the mobile and fixed parts of the mold was modeled by the heat equation:

$$\rho_m C_{p_m}\frac{\partial T}{\partial t} - \lambda_m\frac{\partial^2 T}{\partial x^2} = 0$$

(5)

where $\rho_m$, $C_{p_m}$ and $\lambda_m$ are the density, specific heat and heat conductivity of steel.

Finally, the heat transfer by convection in the cooling circuits was described by:

$$\lambda_m\left[\frac{\partial T}{\partial x}\right]_{x=x_p+x_m} = h_{fluid}\cdot\left[T_{fluid} - T(t, x = x_p + x_m)\right]$$

(6)

The values of the parameters in Equations 1 to 6 used for simulations are listed in Table 1. They were taken from the literature [10, 14, 16] except for the heat capacity, which was measured by differential scanning calorimetry (DSC, Mettler Toledo DSC 1) using a sapphire reference.

**Table 1** Thermophysical and crystallization parameters used for simulations.

| **Mold thermophysical parameters** (1) (Farouq et al., 2005) | **PHBV thermophysical parameters** (2)(Stefani et al., 2009) - (3)Measured by DSC |
|---|---|
| $\rho_m = 7874\left(kg/m^3\right)^{(1)}$ | $\rho = 1200\left(kg/m^3\right)^{(2)}$ |
| $C_{p_m} = 475\left(J/kg/K\right)^{(1)}$ | $\begin{cases} Cp_a = 1990\left(J/kg/K\right) \\ Cp_{sc} = 1.205 \times T + 1612\left(J/kg/K\right)^{(3)} \end{cases}$ |
| $\lambda_m = 45\left(W/m/K\right)^{(1)}$ | $\lambda = 0.156\left(W/m/K\right)^{(2)}$ |
| PHBV crystallization parameters (2) (Stefani et al., 2009) – (4) (Peng et al., 2003) | |
| $\Delta H = 38.3\, kJ/kg^{(2)}$ | $K_g = 3.14 \times 10^5\, K^2\ ^{(4)}$ |
| $G_0 = 4.8090 \times 10^6\ ^{(4)}$ | $T_{m_0} = 175\,°C^{(4)}$ |
| $U^* = 6276\, J/mol^{(4)} \quad n = 3^{(4)}$ | $T_g = 0\,°C^{(4)}$ |

# 3 RESULTS AND DISCUSSION

## 3.1 Flying Probe Temperature Measurements Curves

Figure 4 shows the effect of holding pressure and mold temperature on flying probe temperature measurements $T(t)$ and their time derivative $dT(t)/dt$ curves.

No strong pressure influence can be observed in the studied pressure range. According to previous work on polypropylene crystallization [15], piezo dependence becomes significant above 200 bar. Here, one can observe that pressure influence is only slightly noticeable after the crystallization plateau. This result can be explained by an increase of the polymer's heat conductivity against pressure [19]. More generally, the increase of pressure gives molded part with a greater compactness which enhances as a matter of fact the contact quality between the part and the mold, thus leading to a more rapid cooling.

As an opposition, a strong influence of mold temperature can be observed: raising the mold temperature from 30 to 60 °C delays by roughly 20 s the cooling time necessary to reach a temperature of 80 °C at the core of the PHBV part. The time derivative of the $T(t)$ curves evidences that the molded polymer underwent severe cooling kinetics. Indeed, the cooling rate changes from –250 °C/min to 0 °C/min in less than 15 s for a mold temperature of 30 °C. In the case of the molding achieved under a temperature of 60 °C, one can see that the cooling rate becomes positive, denoting the warming of the part core due to heat released during crystallization.

## 3.2 Simulations and Crystallization Parameters Estimation

Figure 5 shows examples of simulations of experimental data (thick continuous lines) for 2 sets of molding conditions: The first simulations (black dotted lines) are obtained using the parameters available in the literature (Table 1). It can be seen that the simulated cooling curves match qualitatively the cooling kinetics, with the presence of a temperature plateau due to crystallization. However, it clearly fails in predicting the temperature at the crystallization plateau and its duration.

According to our previous work on polypropylene [15], the predictions of the model used for simulations in the crystallization plateau region are extremely sensitive to two parameters: The equilibrium melting temperature $T_{m_0}$ and the latent heat of crystallization $\Delta H$, responsible for the warming of the polymer part. Figure 6 shows a sensitivity study of the model's predictive accuracy with respect to these two parameters: We considered values of $T_{m_0}$ ranging from 170 to 190 °C (around the literature value of 175 °C [10]) and values of $\Delta H$ ranging from 35 to 50 kJ/kg (around the literature value of 38.3 kJ/kg [14]). The plot shows the evolution of the absolute mean square difference $\delta T$ between simulated $T^{sim}$ and measured $T^{exp}$ temperature curves as a function of the two crystallization parameters:

$$\delta T = \sqrt{\frac{1}{m}\sum_{i=1}^{m}(T^{sim}(t_i) - T^{exp}(t_i))^2} \tag{7}$$
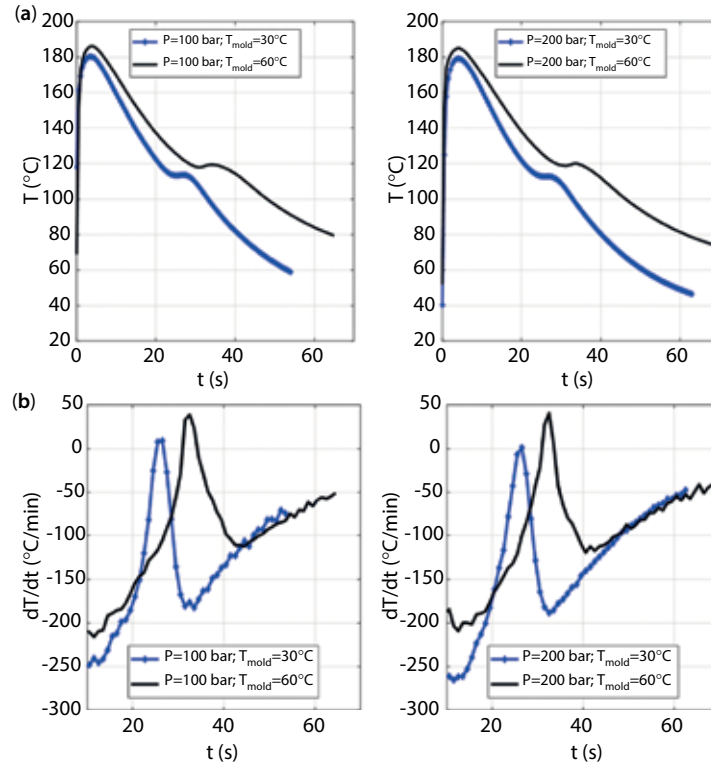
**Figure 4** Flying probe temperature measurements: (**a**) T(t) curves and (**b**) their time derivative dT(t)/dt curves obtained for two holding pressures (100 and 200 bars) and two mold temperatures 30 and 60 °C.
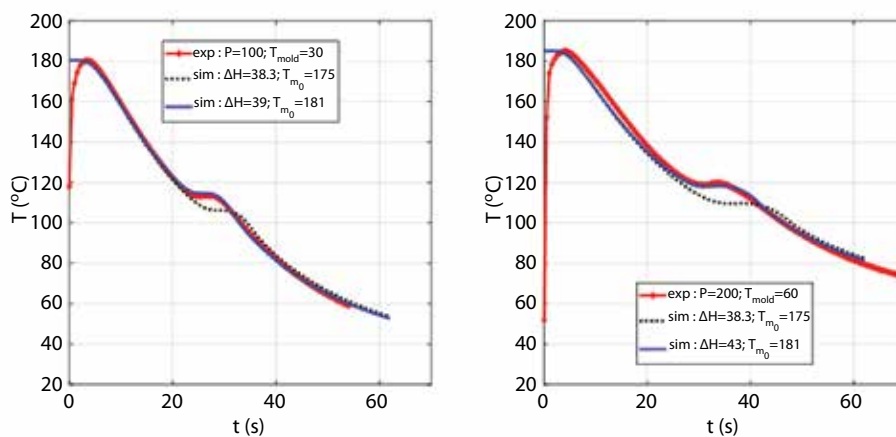


**Figure 5** Simulations vs. experimental data for two sets of molding conditions (pressure, temperature and enthalpy of crystallization are given in bar, °C and kJ/kg, respectively).

where $m$ is the number of considered measurement points acquired at time $t_i$.

One can clearly see in Figure 6 that the values of $T_{m_0}$ which give the best fit for the four molding conditions tested are very close ($180 < T_{m_0} < 182$ °C). Concurrently, the corresponding ΔH values show a relatively more important variation. The heat of crystallization increases by ≈ 10% with both mold temperature and holding pressure from ΔH ≈ 39 kJ/kg

(for 30 °C/100 bar) to ΔH ≈ 43 kJ/kg (for 60 °C/200 bar).

The cooling curves simulations corresponding to these processing conditions with the average value of $T_{m_0}$ ≈ 181 °C and these extreme values of ΔH are plotted on Figure 5. A significantly better fit with experimental data can be observed compared to the initial simulation with fixed literature values (black dotted lines).
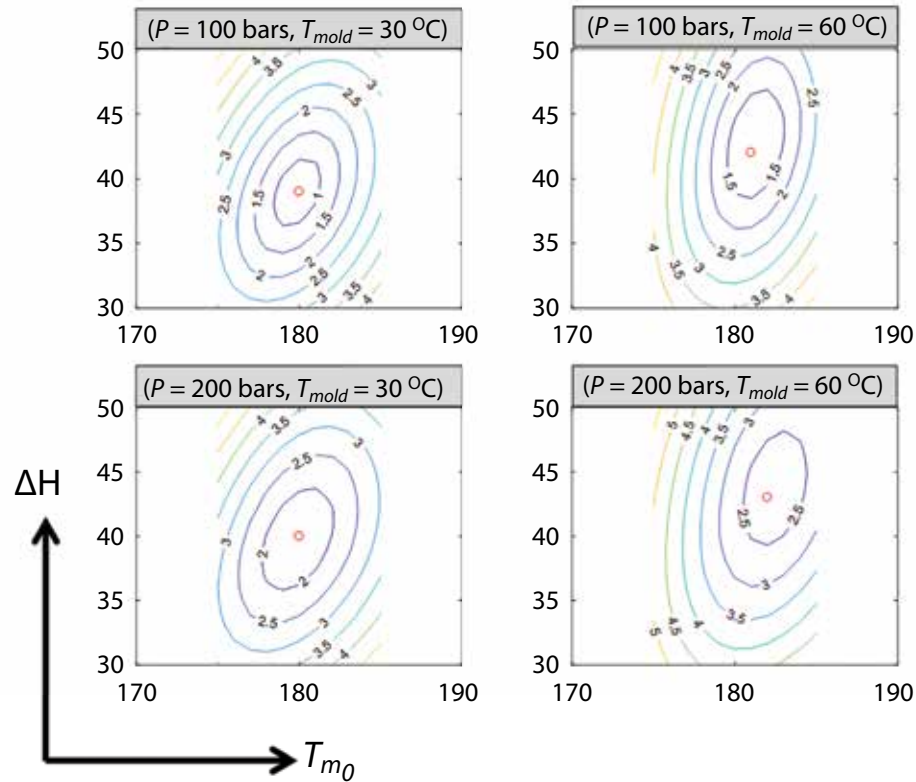
**Figure 6** Influence of $\Delta H$ and $T_{m0}$ values on absolute mean square difference between simulated and measured temperature curves for four molding conditions.

These estimated variations of the estimated latent heat of crystallization can be ascribed to an increase of the final crystallinity of PHBV. It suggests that the processing conditions can modulate the primary crystallization of PHBV. However, as observed in Figure 4, the use of a high mold temperature results in significantly longer cooling times. From an industrial perspective, this is disadvantageous as it affects the productivity of the molding process. In further studies, it may be interesting to try to combine low mold temperature with higher holding pressure values.

## 4 CONCLUSION

In this work we tried to analyze the influence of two injection molding key parameters (holding pressure and mold temperature) on the crystallization of PHBV during the cooling step. Injection tests were carried out in a molding cavity instrumented with pressure sensors and a flying temperature probe located at the middle of the molded part's thickness. These inline temperature measurements were compared to numerical simulations based on the Nakamura crystallization kinetics and the Hoffman-Lauritzen crystallization growth models.

Using the literature values for the thermophysical and crystallization parameters, the simulations describe qualitatively well the cooling behavior of PHBV molded part. A more quantitative prediction was possible by adjusting two key crystallization parameters. Indeed, the resulting estimated value of the equilibrium melting temperature $T_{m0}$ and the latent heat of crystallization $\Delta H$ remain close to the initial literature data but show a 10% variation of $\Delta H$ depending on the processing condition, indicating the possibility to modulate the final crystallinity degree. To our knowledge, this is the first time that these crystallization parameters of PHBV have been estimated under real processing conditions close to industrial use. In particular, the measured cooling rates of the molded parts are shown to be very high compared to offline crystallization experiments done under "much softer" conditions previously reported.

## ACKNOWLEDGMENTS

# REFERENCES

1. E. Bugnicourt, P. Cinelli, A. Lazzeri, and V. Alvarez, Polyhydroxyalkanoate (PHA): Review of synthesis, characteristics, processing and potential applications in packaging. *Express Polym. Lett.* **8**, 791–808 (2014).

2. E. Leroy, I. Petit, J.L. Audic, G. Colomines, and R. Deterre, Rheological characterization of a thermally unstable bioplastic in injection molding conditions. *Polym. Degrad. Stab.* **97**, 1915–1921 (2012).

3. F. Biddlestone, A. Harris, J.N. Hay, and T. Hammond, The physical ageing of amorphous poly(hydroxybutyrate). *Polymer Int.* **39**, 221229 (1996).

4. M. Knights, Injection molding biopolymers: How to process renewable resins. *Plastics Technology* **April** (2009).

5. J. Qian, L.Y. Zhu, J.W. Zhang, and R.S. Whitehouse, Comparison of different nucleating agents on crystallization of poly(3-hydroxybutyrate-co-3-hydroxyvalerates). *J. Polym. Sci. Part B Polym. Phys.* **45**, 1564–1577 (2007).

6. W.H. Kai, Y. He, and Y. Inoue, Fast crystallization of poly(3-hydroxybutyrate) and poly(3-hydroxybutyrate-co-3-hydroxy-valerate) with talc and boron nitride as nucleating agents. *Polymer Int.* **54**, 780–789 (2005).

7. E. Ten, L. Jiang, and M. P. Wolcott, Crystallization kinetics of poly(3-hydroxybutyrate-co-3-hydroxyvalerate)/cellulose nanowhiskers composites. *Carbohydr. Polym.* **90**, 541–550 (2012).

8. G.X. Chen, G.J. Hao, T.Y. Guo, M.D. Song, and B.H. Zhang, Crystallization kinetics of poly(3-hydroxybutyrate-co-3-hydroxyvalerate)/clay nanocomposites. *J. Appl. Polym. Sci.* **93**, 655–661 (2004).

9. X.P. Lu, X. Wen, and D. Yang, Isothermal crystallization kinetics and morphology of biodegradable poly(3-hydroxybutyrate-co-4-hydroxybutyrate). *J. Mater. Sci.* **46**, 1281–1288 (2011).

10. S.W. Peng, Y.X. An, C. Chen, B. Fei, Y.G. Zhuang, and L.S. Dong, Isothermal crystallization of poly(3-hydroxybutyrate-co-3-hydroxyvalerate). *Eur. Polym. J.* **39**, 1475–1480 (2003).

11. W.J. Liu, H.L. Yang, Z. Wang, L.S. Dong, and J.J. Liu, Effect of nucleating agents on the crystallization of poly(3-hydroxybutyrate-co-3-hydroxyvalerate). *J. Appl. Polym. Sci.* **86**, 2145–2152 (2002).

12. Y.X. An, L.S. Dong, Z.S. Mo, T.X. Liu, and Z.L. Feng, Nonisothermal crystallization kinetics of poly(beta-hydroxybutyrate). *J. Polym. Sci. Part B Polym. Phys.* **36**, 1305–1312 (1998).

13. D.A. D'Amico, V.P. Cyras, and L.B. Manfredi, Non-isothermal crystallization kinetics from the melt of nanocomposites based on poly(3-hydroxybutyrate) and modified clays. *Thermochim. Acta* **594**, 80–88 (2014).

14. P.M. Stefani, R.A. Ruseckaite, and A. Vazquez, Poly(3-hydroxybutyrate-co-11 mass%3-hydroxyvaleate) molded part during the solidification step. *J. Therm. Anal. Calorim.* **95**, 305–312 (2009).

15. M.C. Le, S. Belhabib, C. Nicolazo, P. Vachot, P. Mousseau, A. Sarda, and R. Deterre, Pressure influence on crystallization kinetics during injection molding. *J. Mater. Process. Technol.* **211**, 1757–1763 (2011).

16. Y. Farouq, C. Nicolazo, A. Sarda, and R. Deterre, Temperature measurements in the depth and at the surface of injected thermoplastic parts. *Measurement* **38**, 1–14 (2005).

17. S. Peng, Y. An, C. Chen, B. Fei, Y. Zhuang, and L. Dong, Isothermal crystallization of poly(3-hydroxybutyrate-co-3-hydroxyvalerate). *Eur. Polym. J.* **39**, 1475–1480 (2003).

18. K. Nakamura, K. Katayama, and T. Amano, Some aspects of nonisothermal crystallization of polymers. II. Consideration of the isokinetic condition. *J. Appl. Polym. Sci.* **17**, 1031–1041 (1973).

19. A. Dawson, M. Rides, and J. Nottay, The effect of pressure on the thermal conductivity of polymer melts. *Polym. Test.* **25**, 268–275 (2006).